

Accurate estimation of fish length in single camera photogrammetry with a fiducial marker

Monkman, Graham G; Hyder, Kieran; Kaiser, Michel J; Vidal, Franck P

ICES Journal of Marine Science

DOI:
[10.1093/icesjms/fsz030](https://doi.org/10.1093/icesjms/fsz030)

Published: 01/11/2020

Peer reviewed version

[Cyswllt i'r cyhoeddiad / Link to publication](#)

Dyfyniad o'r fersiwn a gyhoeddwyd / Citation for published version (APA):
Monkman, G. G., Hyder, K., Kaiser, M. J., & Vidal, F. P. (2020). Accurate estimation of fish length in single camera photogrammetry with a fiducial marker. *ICES Journal of Marine Science*, 77(6), 2245-2254. <https://doi.org/10.1093/icesjms/fsz030>

Hawliau Cyffredinol / General rights

Copyright and moral rights for the publications made accessible in the public portal are retained by the authors and/or other copyright owners and it is a condition of accessing publications that users recognise and abide by the legal requirements associated with these rights.

- Users may download and print one copy of any publication from the public portal for the purpose of private study or research.
- You may not further distribute the material or use it for any profit-making activity or commercial gain
- You may freely distribute the URL identifying the publication in the public portal ?

Take down policy

If you believe that this document breaches copyright please contact us providing details, and we will remove access to the work immediately and investigate your claim.

Accurate estimation of fish length in single camera photogrammetry with a fiducial marker

Graham G. Monkman ^{a,*}, Kieran Hyder ^{d,e}, Michel J. Kaiser ^{a,c}, Franck P. Vidal ^b

^a School of Ocean Sciences, Bangor University, Menai Bridge, Anglesey LL59 5AB, United Kingdom

^b School of Computer Science, Bangor University, Menai Bridge, Anglesey LL59 5AB, United Kingdom

^c Marine Stewardship Council, Marine House, 1 Snow Hill, London EC1A 2DH

^d Centre for Environment, Fisheries & Aquaculture Science, Pakefield Road, Lowestoft, Suffolk NR33 0HT, United Kingdom

^e School of Environmental Sciences, University of East Anglia, Norwich Research Park, Norwich, Norfolk NR4 7TJ, United Kingdom. Tel. +44 (0)1502 524501

* Corresponding author at: School of Ocean Sciences, Bangor University, Menai Bridge, Anglesey LL59 5AB, United Kingdom. Tel.: + 44 (0)1248 382842.

Email addresses: gmonkman@mistymountains.biz (G.G. Monkman); michel.kaiser@msc.org (M.J. Kaiser), kieran.hyder@cefas.co.uk (K. Hyder); f.vidal@bangor.ac.uk (F.P. Vidal)

ORCID

G.G. Monkman <http://orcid.org/0000-0002-5645-1834>, K. Hyder <http://orcid.org/0000-0003-1428-5679>, M. J. Kaiser <http://orcid.org/0000-0001-8782-3621>, F.P. Vidal <https://orcid.org/0000-0002-2768-4524>

Keywords fiducial marker, image distortion, OpenCV, photogrammetry, single camera, total length estimation

Abstract

Videogrammetry and photogrammetry are increasingly being used in marine science for unsupervised data collection. The camera systems used to collect such data are varied and often complex. In contrast, digital cameras and smartphones are ubiquitous, convenient for the user and an image automatically captures much of the data normally recorded on paper as metadata. The limitations of such an approach are primarily attributed to errors introduced through both the image acquisition process and lens distortion of the collected images. In the present study, a methodology is presented to achieve accurate 2-dimensional (2-D) total length (TL) estimates of fish without specialist camera equipment or proprietary software. Photographs of depressed (flat) and fusiform fish were captured with an action camera using a background fiducial marker, positioned at the distal plane of the subject; a foreground fiducial marker, at the proximal plane of the subject and a laser marker, projected on to the subject's surface. To correct image distortions, the geometric properties of the lens were modelled with OpenCV. The accuracy of TL estimates were corrected for parallax effects using a novel iterative algorithm requiring only the initial length estimate and known morphometric relationships. OpenCV was effective in correcting image distortion, decreasing RMSE by 96% and the percentage mean bias error (%MBE) by 50%. By undistorting the image and correcting for parallax effects a % MBE [95% CIs] of -0.6% [-1.0, -0.3] was achieved and RMSE was reduced by 86% to 2.1%. Estimation of the lens to subject distance using the similar triangles calibration method resulted in the best estimation of TL. The present study demonstrates that the morphometric measurement of different species can be accurately estimated without the need for expensive, complex or bulky camera equipment making it particularly suitable for deployment in citizen science and other volunteer based data collection endeavours.

1 Introduction

Cost reductions and advances in camera equipment and supporting technologies (e.g. durability, storage and computing capacity, connectivity, and supporting software) are stimulating research and development into the applications of photogrammetry and videogrammetry (hereafter referred to as photogrammetry) to marine research (Bicknell, Godley, Sheehan, Votier, & Witt, 2016; Struthers, Danylchuk, Wilson, & Cooke, 2015). Potential applications include remote electronic monitoring (virtual observation) of commercial fisheries to assess catch (e.g. White *et al.*, 2006; Chang *et al.*, 2010; Hold *et al.*, 2015; Bartholomew *et al.*, 2018) and bycatch (e.g. Bartholomew *et al.*, 2018), ecological studies using fixed cameras (e.g. Bouchet and Meeuwig, 2015; Schmid *et al.*, 2017), direct observational surveys (e.g. Harvey *et al.*, 2001, Jaquet, 2006), behavioural studies (e.g. Nguyen *et al.*, 2014, Claassens and Hodgson, 2018) and in aquaculture (e.g. Costa *et al.*, 2006).

Length data is particularly important in the assessment of fish stocks in recreational and commercial capture fisheries (Pauly & Morgan, 1987) however, the collection of length measurements is time consuming and costly. Photogrammetry can increase throughput (Chang *et al.*, 2010), mitigate against factors such as observer biases (Faunce & Barbeaux, 2011; Harvey *et al.*, 2001), and be more cost-effective per data point acquired than manual at-sea length observations and length sampling (Chang *et al.*, 2010; National Oceanic and Atmospheric Administration, 2015a, 2015b).

The equipment typically deployed for photogrammetry includes multiple parallel lasers (e.g. Deakos, 2010; Rogers *et al.*, 2017; Bartholomew *et al.*, 2018) and/or multiple cameras (e.g. Dunbrack, 2006; Rosen *et al.*, 2013; Neuswanger *et al.*, 2016). In parallel laser systems the lasers create a visible fiducial marker of known length at the surface of the subject of interest. When the plane of the subject surface is aligned with the plane of the camera sensor then the actual length represented by an image pixel will be invariant across the subject provided the

image and the subject are not distorted. Under these assumptions an accurate length estimate can be made. Multi-camera systems are mathematically more complex, but allow 3-dimensional subject length (and other measures) to be estimated using triangulation methods (e.g. Neuswanger *et al.*, 2016). Accurate length estimates have also been derived by deployment of a simpler system by analysing images captured with a single camera and a physical fiducial marker of known length (Hold et al., 2015; van Helmond, Chen, & Poos, 2017).

Photogrammetry has the potential to widen the participation of non-scientists as novel sources of data. Citizen science projects can use smartphone applications to improve engagement with participants (reviews Hyder et al., 2015, Venturelli et al., 2017) and can be utilised for species identification from images captured using smartphones (Fishbrain, 2018). The assessment of marine recreational fisheries (MRF)—which can be data poor even in developed countries (ICES, 2017)—may particularly benefit from the deployment of simple photogrammetry solutions. Surveys of MRF frequently have a diary phase in which anglers record details of their catch (ICES, 2017). Volunteer based assessments may be the best means of collecting longitudinal data under budgetary limitations.

To accurately estimate length from images using a fiducial marker several corrections are necessary. Cameras have different intrinsic tangential distortion, where the sensor plane is not perpendicular to the optical axis. Additionally, the wide-angle lenses—typical of action cameras and smartphones—exhibit radial distortion. These factors introduce systematic length estimation errors as the actual length represented by pixels across the captured image plane varies with the location of the pixel in the image. Any estimation of actual size can be biased by the increasing depth and aspect between the subject, the fiducial marker and the camera (*parallax effect*). Camera calibration is well understood (see Szeliski, 2010 pp288-295) nonetheless, correcting fiducial marker-made length estimates for subject aspect in single

camera systems has received little research attention. Optical corrections can be made using the thin-lens equation provided the lens to subject distance is known. However, measuring the lens to subject distance is impractical for some uses, such as in volunteer based projects where the volunteer could not be expected to accurately measure the lens to subject distance each time an image was captured.

This study aims to introduce a methodology to minimise errors in morphometric measurements of fish (and other organisms) when using single camera photogrammetry. The methodology is particularly relevant to the automation of length extractions in machine vision pipelines for volunteer led applications used in the assessment of recreational fisheries or small scale and developing artisanal or commercial fisheries. The objectives are to (i) empirically compare the accuracy of low-cost foreground, background and laser fiducial markers; (ii) validate the effectivity of OpenCV in correcting intrinsic lens distortion in any camera; (iii) describe methods to minimise error in length estimates made with fiducial markers; and (iv) compare the effectiveness of applying a lens distortion correction and parallax correction without prior knowledge of the lens to subject distance.

2 Methods

2.1 Image acquisition and actual TL measurement

Two species of fish with different body shape were selected to support the generalisability of the presented methodology. The European sea bass is a pelagic predator with fusiform body shape (i.e. roughly cylindrical in cross section and tapers towards the ends). Conversely, the common dab is a flat fish with a depressed body shape. Photographs of euthanised European sea bass (*Dicentrarchus labrax*, $n = 43$) were gathered *in-situ* at two commercial fish processors in North West Wales, UK in November 2016 and March 2017. Images of common dab (*Limanda limanda*, $n = 32$) were captured at the School of Ocean Sciences laboratory, Bangor University, UK in January 2017. The camera system was a Nextbase 512G camera encased in

a custom waterproof housing fitted with a 12v battery. The Nextbase 512G optical system has a wide angled field of view (FoV) and significant barrel distortion, which allowed the effectiveness of lens distortion correction to be evaluated. To provide stability the camera housing was mounted on a Manfrotto 244 variable friction arm and bracket. Projective distortion was minimised by using spirit levels to ensure the principle lens plane and the surface on which the photographic subject lay were parallel.

The camera was set to record video at 30 frames per second and a resolution of 1280×720 pixels. Video capture—as opposed to single frame photographs—was used to minimise perturbation to the camera.. The distance between the surface on which the fish lay and the front of the camera housing was measured with a 1 m steel rule (required for depth adjustment as outlined later). The total length (TL) of the fish (i.e. the distance between the tip of the snout to the tip of the caudal fin) was measured using a fish measuring board with the caudal lobes pushed gently together and then allowed to settle without further coercion. All measuring rules were validated with a rule certified to an accuracy of 0.9998%. Throughout the manuscript, all lengths refer to TL unless otherwise specified.

The precision and accuracy of the three types of fiducial markers were compared (Fig. 1), these were; (i) marker positioned at the backplane (*distal plane*) of the subject (henceforth *background marker*); (ii) paired lasers projected onto the near surface of the subject (henceforth *laser marker*); and (iii) a marker positioned on the fish surface (*proximal plane*) closest to, and parallel with, the plane of the camera lens (henceforth *foreground marker*).

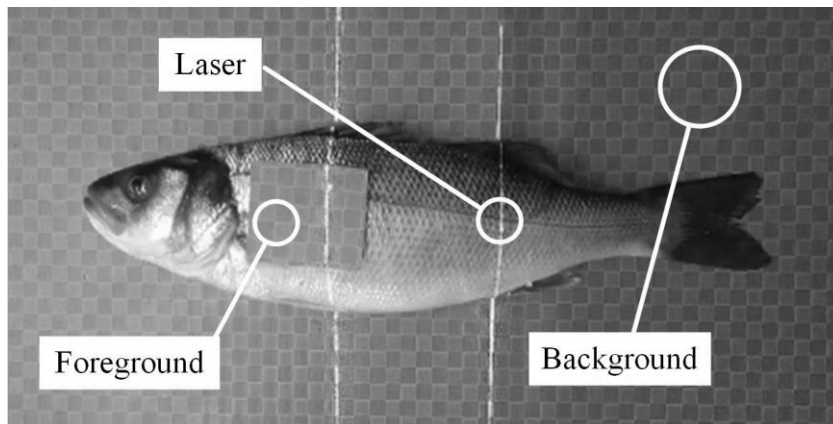


Fig. 1. Placement of the three fiducial markers on a European sea bass. The checkerboard cell scale is 1 cm².

The foreground and background markers were a checkerboard of 1 cm² cells mounted on a flat polycarbonate sheet (Fig. 1). The laser marker used two parallel-paired lasers (Odiforce, 3-5mW Green Laser Module) mounted inside the camera housing. The distance between the laser markers at the midpoint of the fish depth was recorded manually because the laser lines were not parallel at the scale of interest due to fabrication errors when seating the lasers within the custom camera housing.

Still JPEG images were extracted from the video using VLC media player (VideoLAN, 2018). TL estimates were made from the still images using ImageJ (Schneider et al., 2012) for each of the 3 fiducial markers. The background fiducial marker actual length per pixel (ALPP) was calculated across the total fish length. The pixel length of the fish was measured in the image by the line segment joining the tip of the snout through the centre of the caudal peduncle and the fork to the intersection with the imaginary line between the tips of the caudal fin.

2.2 Hierarchy of length correction refinements

The position of each fiducial marker type in relation to the camera is shown in Fig. 2. It is apparent that the estimation of the ALPP is dependent on the distance between the fiducial marker and the camera. The actual length is invariant however, the size of marker image formed on the camera sensor increases as the object to lens distance decreases. Errors in TL estimation

arise because of variation in the distance between the fiducial markers and the fish profile. Measurement errors are also caused by image distortion arising from the geometric properties of the camera-lens system (henceforth *intrinsic camera properties*, as commonly known in the field). To obtain accurate TL estimates, these two sources of error need to be corrected.

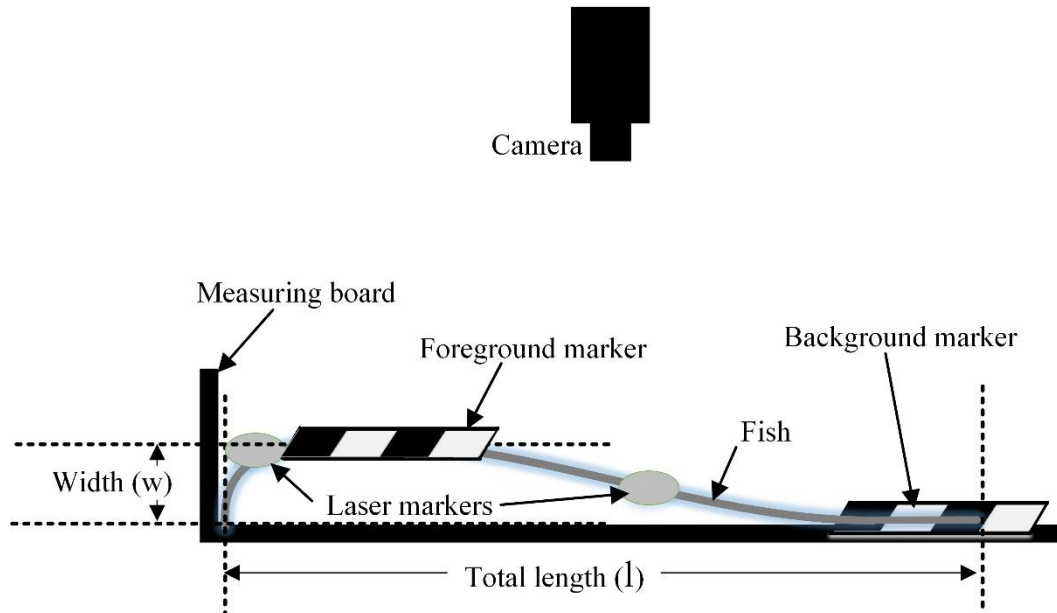


Fig. 2. Schematic showing the measurement of total fish length, and the relative position of foreground, background and laser fiducial markers to the camera. Width describes the elevation of the fish above the distal plane.

2.3 Correcting for image distortion

To correct for tangential distortion, radial distortion and lens misalignment, the intrinsic parameters of the camera at a fixed zoom (focal length) and the lens distortion coefficients need to be calculated (Szeliski, 2010). Multiple images of a regular 2D pattern were captured in different orientations and the intrinsic camera matrix and distortion coefficients calculated using Python 3.5 and OpenCV (OpenCV team, 2018). This camera profile is saved and can then be reused to undistort images taken with the same camera for a given focal length. Supplementary materials A lists the code used for camera profile creation and undistorting images.

The efficacy of the distortion correction was estimated by photographing a checkerboard pattern and manually marking the vertices both before and after distortion correction. On an

image without radial distortion, the vertices of a checkerboard row or column lie on straight line, therefore the x and y coordinates were regressed and the residuals used to calculate the Euclidean distance in pixels of the marked point from the idealised vertex. The root mean squared error (RMSE) was calculated for each horizontal and vertical line of vertices and 1st and 2nd order statistical moments calculated across images. RMSE for a given line is given by $RMSE = (\sum_{i=1}^n (e_i - o_i)^2 / n)^{1/2}$. where e_i is the i^{th} expected Euclidean distance of the marked point from the idealised vertex (i.e. 0 pixels) and o_i is the i^{th} *actual* Euclidean distance of the distorted vertex from the idealised vertex.

Errors arising from positional differences between fish and camera were minimised by ensuring the camera and fish were aligned as previously described and ensuring the subject was placed on the background marker with minimal body distortion. Henceforth TL estimates taken from an undistorted image are known as *undistorted TL*.

2.4 Correcting for subject profile

In the case of the laser and foreground markers, the width of a fusiform fish (w , Fig. 2) causes an underestimate of the ALPP, therefore TL (l , Fig. 2) is also an underestimate. TL estimations made with a foreground marker were corrected using a well-known manipulation of the thin lens equation where $a = b(1 - w)/d$ (Fig. 3).

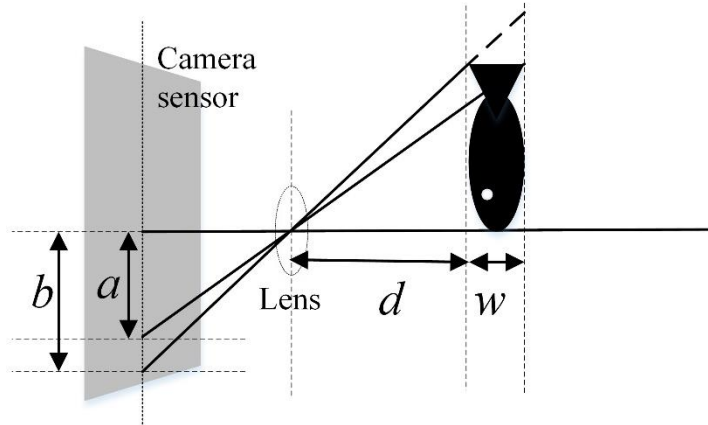


Fig. 3. Schematic describing the thin-lens model, which relates actual object lengths to image formation at the camera sensor.

This correction (henceforth *depth corrected TL*) can be interpreted as having adjusted the ALPP to be the same as if the foreground fiducial marker was positioned at the distal plane. To calculate *depth corrected TL*, the width of the fish is required, which can be estimated from the length, provided the length-width relationship is known (Jeong, Yang, Lee, Kang, & Lee, 2013; Loy, Boglione, Gagliardi, Ferrucci, & Cataudella, 2000; Rohlf & Marcus, 1993; Tulli, Balenovic, Messina, & Tibaldi, 2009). However, *depth corrected TL* is subject to systematic error because the estimated length used to derive width is itself an underestimate. This underestimate occurs because the ALPP is calculated from the foreground fiducial marker dimensions, which is nearer the camera lens than a significant proportion of the fish body. To address this, TL was corrected iteratively according to the process shown in Fig. 4. This correction is described as *iterative corrected TL*, using the following equation; $l_{und} + l_{cor}$ where l_{cor} is the sum of iteratively calculated lengths larger than a minimum threshold (Supplementary materials C).

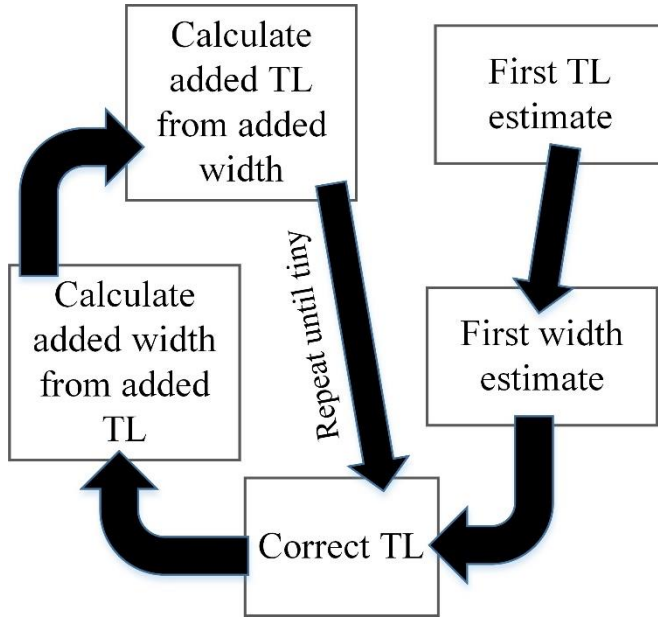


Fig. 4. Iterative process to improve accuracy of total length (TL) estimates. TL and widths are estimated using the morphometric relationship between the two dimensions.

Iterative corrected TL does not account for the varying width profile of the fish between the proximal and distal subject planes. To test this correction methodology, we compared two different body shapes using common dab and European sea bass and calculated the mean width (mm) for each species. Mean widths were measured by bisecting fish through the long axis of the coronal plane. Bisected samples were then photographed against a white background. Images were thresholded (i.e. subject pixels set to white, background pixels set to black), then the standardised mean width \hat{w} was derived from the mean pixel width across the thresholded images (Fig. 5), according to $\hat{w} = (1/n \cdot \sum_1^n w_i) / \max(w_i)$ where n is the number of pixel columns and w_i is the height in pixels of the i^{th} column. This factor was used to correct the *iterative corrected TL* to derive the *profile corrected TL* (l_p) according to $l_p = \hat{w} \cdot l_{cor} + l_{und}$. (Supplementary materials B).

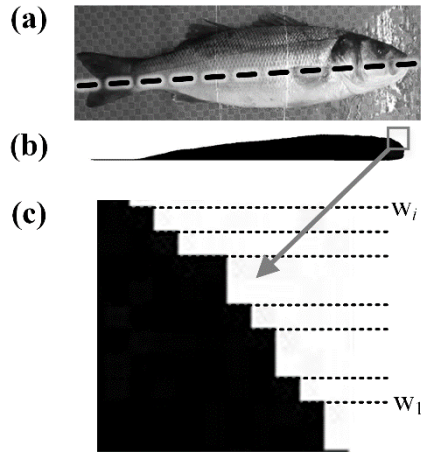


Fig. 5. Fish were bisected through the coronal plane (a), and the width profile photographed against a white background. The image was then thresholded (b) and the mean pixel width calculated (c).

2.5 Estimation of TL when the distance between lens and fish is unknown

Length corrections derived from the thin lens equation require prior knowledge of the distance between the lens and fish. This is impractical for applications where experimental control is not possible. Two methods based on the thin lens model can be used to estimate d if a fiducial marker appears in the image. Firstly, d can be estimated if we know some of the camera properties, according to $d = (f \cdot h \cdot \acute{s})/(\acute{h} \cdot s)$ where f is the focal length, h is the actual size of the fiducial marker, \acute{s} is the sensor height in pixels, \acute{h} is the height of the fiducial marker in pixels and s is the actual size of the sensor. Secondly, d can be estimated by taking one (or more) calibration images with a marker of known length, according to $d = (h_c \cdot h \cdot f)/(\acute{h}_c \cdot \acute{h})$, where f is the focal length, h_c is the actual size of the calibration marker, h is the actual size of the fiducial marker, \acute{h}_c is the height in pixels of the calibration marker and \acute{h} is the height of the fiducial marker in pixels.

Both methods were used to estimate d (Fig. 3) in the calculation of the *profile corrected TL* and are reported as *calibrated profile corrected TL* and *sensor profile corrected TL*. Supplementary materials C lists the core functions used to produce these corrections. In summary, the mean bias error (MBE) is reported for the variables listed in Table 1. Mean bias

error (MBE) is calculated according to $MBE = 1/n \cdot \sum_{i=1}^n \hat{y}_i - y_i$, where \hat{y}_i is the i^{th} estimate of the *actual TL* y_i . Percent MBE is given by $\%MBE = 100/n \cdot \sum_{i=1}^n \hat{y}_i - y_i/y_i$.

Table 1. Description of variables used in this article.

Variable	Derived From	Comment
<i>Actual TL (l)</i>	N/A	TL measured using a fish board
<i>Distorted TL</i>	Distorted image	TL estimated from an image without any correction for lens distortion
<i>Undistorted TL</i>	Undistorted image	TL estimated from an undistorted image, reported for all three fiducial marker types.
<i>Depth corrected TL</i>	Undistorted TL	Adjustment for the difference in the distance between the proximal and distal plane of the subject. Not applicable for the background marker. Uses the actual lens subject distance in the calculation.
<i>Iterative corrected TL</i>	Depth corrected TL	Apply an adjustment for the initial underestimate of TL.
<i>Profile corrected TL</i>	Iterative corrected TL	Apply an adjustment accounting for the mean profile width of the subject, i.e. correcting for the parallax effect.
<i>Calibrated profile corrected TL</i>	Depth corrected TL	Recalculates depth corrected TL using an estimate of the lens to subject distance using similar triangles, then applies the same process used to calculate the profile corrected TL.
<i>Sensor profile corrected TL</i>	Depth corrected TL	Recalculates the depth corrected TL based on the thin lens equation parameterised with camera properties, then applies the same process used to calculate the profile corrected TL.

2.6 Statistical Analysis

Homogeneity of variance was determined using Levene's test. Where data were heterogeneous, estimators of central tendency were calculated using a 1000 sample bias corrected accelerated bootstrap (BCA) in SPSS (IBM Corp, 2011). Note that 95% confidence intervals are quoted in results (in square brackets) unless otherwise stated.

242 A weighted least squares general linear mixed model (wls-GLMM) was used to compare
 243 percent errors ($e_{\%}$) for the species (random) and marker (fixed) factors. The vector of weights
 244 (\mathbf{w}) were calculated as follows. Let $|\mathbf{r}|$ be the vector of absolute non-standardized residuals from
 245 the regression $e_{\%} \sim \text{species} + \text{marker} + \text{species} * \text{marker}$. Then let \mathbf{p} be the vector of
 246 predicted values of $|\mathbf{r}| \sim \text{species} + \text{marker} + \text{species} * \text{marker}$. Then the vector of
 247 weights \mathbf{w} , is $\mathbf{w} = 1/\mathbf{p}^2$.

248 **3 Results**

249 **3.1 Size ranges**

250 European sea bass sizes ranged between 279 mm and 580 mm (Fig. 6a), and common dab
 251 between 100 mm to 282 mm (Fig. 6b). For European sea bass, the length-width relationship
 252 was taken from data published in Poli et al. (2001) to give $\text{width} = 0.136 \cdot \text{total length} -$
 253 0.367 , where length is measured in centimetres. For common dab ($n = 21$) $\text{width} = 0.087 \cdot$
 254 $\text{total length} - 2.915$ ($R = 0.98$, $p < 0.001$). The standardised mean widths (a proportion)
 255 were estimated as 0.598 and 0.505 for European sea bass and common dab respectively.

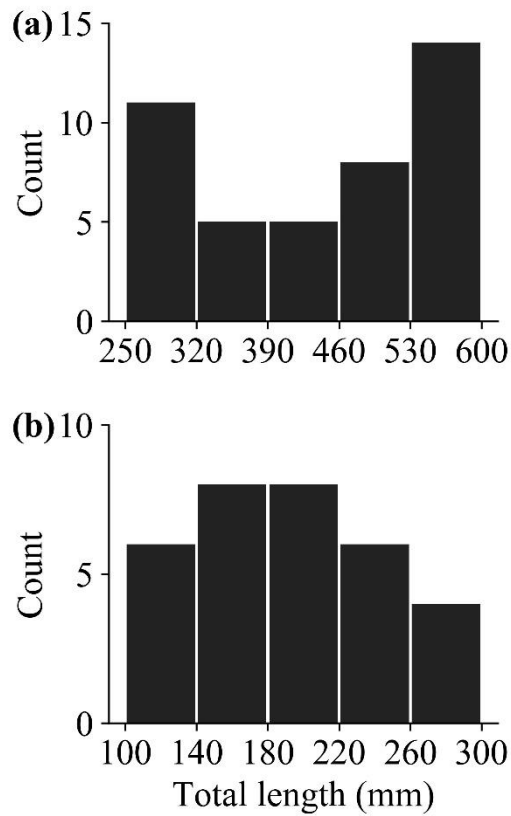


Fig. 6. Actual total length histograms for European sea bass (a) and common dab (b). N.B. y-axis scales differ.

3.2 Distortion correction

OpenCV (OpenCV team, 2018) was successful in reducing the radial distortion of the optical system of the NextGen 512G camera (Fig. 7). In captured images a pixel represented distances of between 0.5 mm and 1.0 mm. The absolute deviation of the vertices from idealised straight lines in distorted images was mean \pm SD 18.2 pixels \pm 11.3 compared to a mean \pm SD of 0.7 pixels \pm 0.4 for the undistorted images and RMSE was reduced by 96% (distorted RMSE = 21.4 pixels, undistorted RMSE = 0.76 pixels).

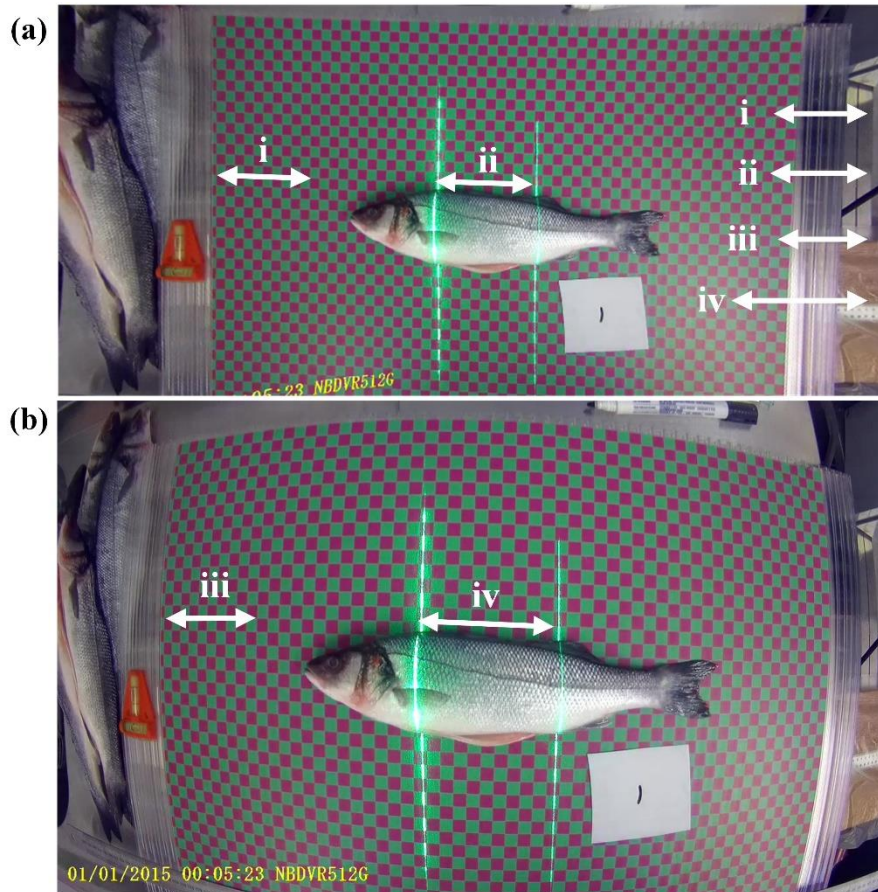


Fig. 7. Example image of European sea bass, with radial distortion (a) and without distortion (b). The lines i, ii, iii and iv were set at 10 cm against the background fiducial marker.

3.3 Distortion corrected length estimates

The laser and foreground fiducial markers substantially underestimated *actual TL* in both species without lens correction for laser and foreground markers (Fig. 8; Table 2; aggregated %MBE = -12.9% [-14.1, -11.7]) and this bias was still substantial for laser and foreground markers after distortion correction (Fig. 8; Table 2; *undistorted TL*, aggregated %MBE = -6.5% [-7.1, -5.9]). Estimations made using the background marker were comparatively accurate, precise and robust to lens distortion however, TL was slightly overestimated in both species (Fig. 8; Table 2; aggregated %MBE = 2.4% [2.1, 2.7]). Undistorting the images improved background MBE by just 0.6 mm for European sea bass and 0.7 mm for common dab (aggregated %MBE = 2.3% [1.9, 2.7]).

In common dab the magnitude of the absolute error [*modulus*(estimate total length - *actual TL*)] increased linearly with fish size for all marker types (Fig. 8b, BCA bootstrap linear

275 regression, $p < 0.05$). However, in European sea bass the error increase did not occur when TL
 276 estimates were made with the foreground marker (Fig. 8a, BCA bootstrap linear regression,
 277 $p > 0.05$). It is apparent that the systematic linear increase in error was most marked in
 278 estimates of common dab TL and with the laser marker (Fig. 8b).

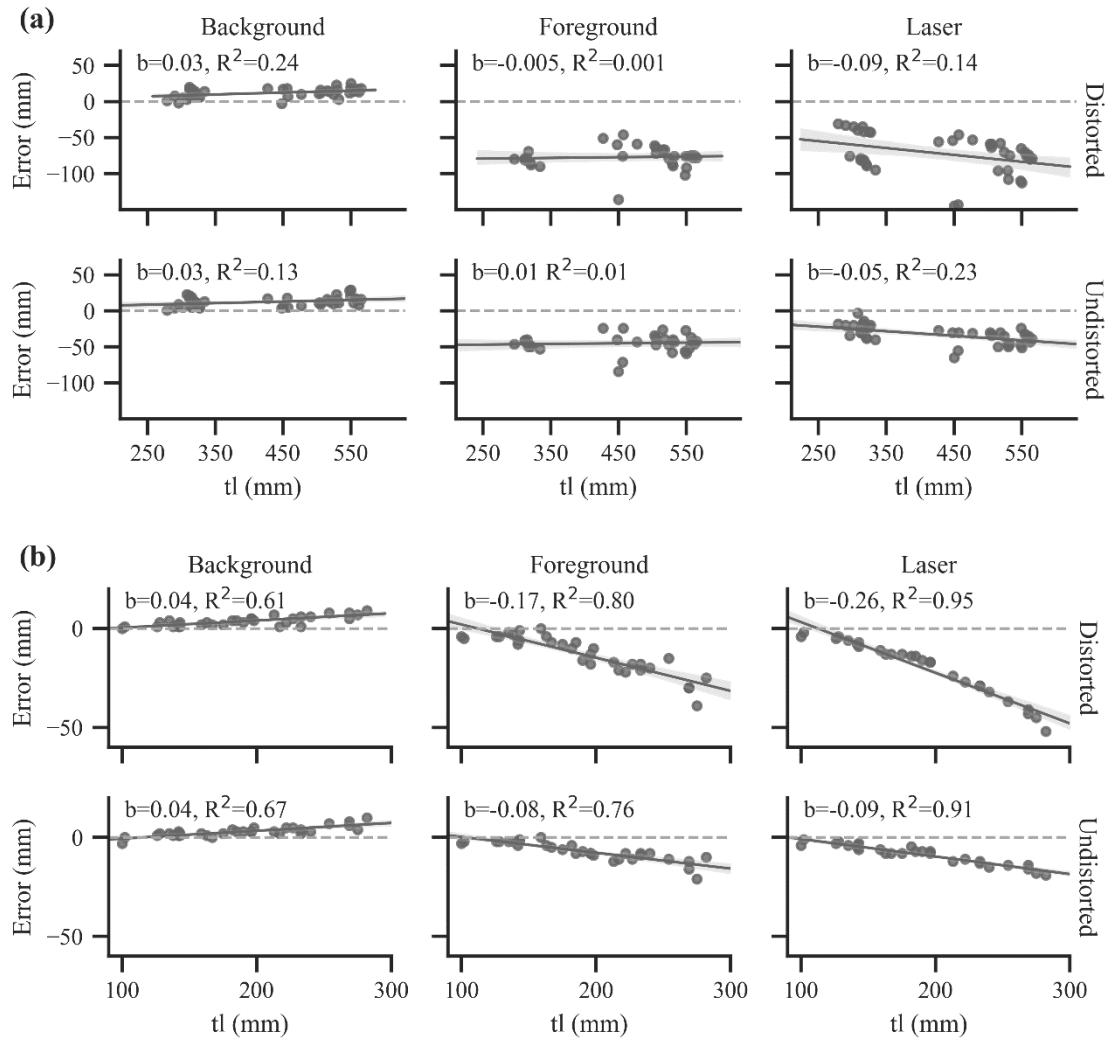


Fig. 8. Error in estimation of total length (tl) for European sea bass (a) and common dab (b) using foreground, background and laser fiducial markers from images without correction of radial and tangential distortion (distorted) and after correcting images for distortion (undistorted). Plot is *actual TL* measured using a fish board vs. (corrected total length - *actual TL*). A negative error represents an underestimate of total length. Shaded lines are 95% confidence intervals. Linear regression coefficient (b) and R^2 reported. Bootstrapped ($n = 1000$) confidence intervals are shown as shaded lines. N.B. y-axis scales differ between species.

279 3.4 Length estimate refinements

280 Applying successive width profile corrections to images substantially improved accuracy for
 281 both species when compared to *undistorted TL* (Fig. 9) in both species, with an overall

282 reduction in %MBE of 95% (i.e. -12.9% to -0.6%). *Profile corrected TL* had the greatest
 283 accuracy and lowest variance (Fig. 9, Table 2) with an aggregated mean %MBE of -0.6%
 284 [-1.0, -0.3] and RMSE was reduced by 86% from 14.8% to 2.1%. In both species, *profile*
 285 *corrected TL*, *calibrated profile corrected TL* and *sensor profile corrected TL* suppressed error
 286 scaling with increasing TL when compared with non-profile based corrections. This effect is
 287 indicated by the reduced magnitude of the linear regression coefficients across the various
 288 profile corrections (Fig. 9; ANOVA, $F_{(1, 28)} = 6.26$, $p = 0.02$, $\eta^2 = 0.19$).

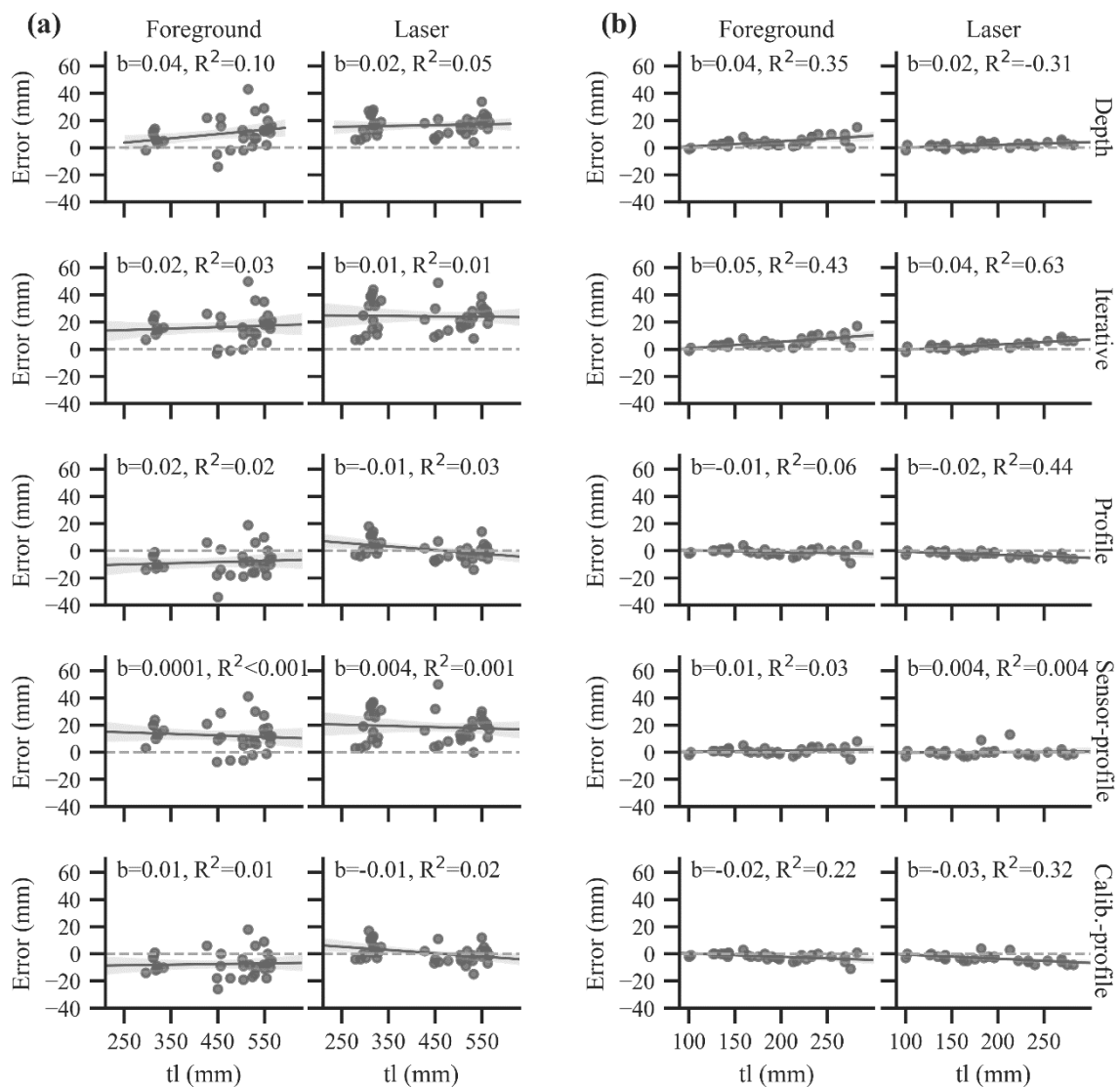


Fig. 9. Error in estimation of total length (tl) for European sea bass (a) and common dab (b), using foreground and laser fiducial markers after correcting images for lens distortion. Plot is *actual TL* measured using a fish board vs. (corrected total length - *actual TL*). A negative error represents an underestimate of total length. Linear regression coefficient (*b*) and R² reported. Bootstrapped ($n = 1000$) confidence intervals are shown as shaded lines.

Table 2. Mean bias errors (MBE) \pm standard deviation (SD) and 95 % confidence intervals (CIs) for 7 different total length estimates variables calculated using background, foreground and laser fiducial markers from images of European sea bass and common dab. All measurements are given in mm.

	Background				Foreground				Laser			
	<i>n</i>	MBE \pm SD	Range	95% CIs	<i>n</i>	MBE \pm SD	Range	95% CIs	<i>n</i>	MBE \pm SD	Range	95% CIs
European sea bass (<i>Dicentrarchus labrax</i>)												
Distorted	43	12.8 \pm 6.9	-3 – 27	10.9 – 14.7	35	-78.5 \pm 16.3	-136 – -46	-83.8 – -73.5	43	-73.2 \pm 26.8	-145 – -31	-81.6 – -65.2
Undistorted	43	13.3 \pm 7.9	1 – 39	11.1 – 15.6	35	-44.7 \pm 13.2	-84 – -23	-48.9 – -40.5	43	-33.3 \pm 12.3	-65 – -3	-36.9 – -29.8
Depth	-	-	-	-	35	11.4 \pm 11.7	-14 – 43	7.6 – 15.4	43	18.0 \pm 10.0	4 – 55	15.3 – 21.1
Iterative.	-	-	-	-	35	17.5 \pm 12.0	-3 – 50	13.6 – 21.7	43	25.8 \pm 13.2	7 – 69	22.2 – 29.9
Profile	-	-	-	-	35	-7.5 \pm 10.9	-34 – 19	-10.8 – -4.2	43	2.0 \pm 9.0	-14 – 31	-0.4 – 4.8
Sensor profile	-	-	-	-	35	13.2 \pm 11.3	-7 – 41	9.5 – 17.1	43	20.0 \pm 13.1	0 – 58	16.6 – 23.6
Calibration profile	-	-	-	-	35	-6.7 \pm 10.0	-26 – 18	-9.8 – -3.5	43	1.7 \pm 8.8	-15 – 30	-0.8 – 4.6
Common dab (<i>Limanda limanda</i>)												
Distorted	32	3.7 \pm 2.4	0 – 9	2.9 – 4.5	32	-12.9 \pm 9.7	-39 – 0	-16.0 – -10.3	28	-19.3 \pm 14.2	-52 – -2	-24.4 – -15.0
Undistorted	32	3.0 \pm 2.5	-3 – 10	2.2 – 3.8	32	-6.8 \pm 4.8	-21 – 0	-8.5 – -5.3	28	-8.6 \pm 5.0	-19 – -1	-10.3 – -7.1
Depth	-	-	-	-	32	4.3 \pm 3.5	-1 – 15	3.2 – 5.4	28	1.9 \pm 1.9	-2 – 6	1.2 – 2.5
Iterative	-	-	-	-	32	4.9 \pm 3.9	-1 – 17	3.8 – 6.1	28	2.9 \pm 2.6	-2 – 9	2.1 – 3.8
Profile	-	-	-	-	32	-0.8 \pm 2.6	-9 – 4	-1.9 – .1	28	-2.7 \pm 1.9	-6 – 0	-3.4 – -2.1
Sensor profile	-	-	-	-	32	1.1 \pm 2.5	-5 – 8	0.2 – 2.1	28	0.1 \pm 3.4	-3 – 13	-1.1 – 1.6
Calibration profile	-	-	-	-	32	-1.9 \pm 2.6	-11 – 3	-3.0 – -1.0	28	-3.2 \pm 2.9	-8 – 4	-4.3 – -2.2

Of the two profile corrections which used an estimation of subject-lens distance, *calibrated profile corrected TL* had a higher degree of accuracy (*calibrated profile corrected TL*, %MBE, $M = -0.8\%$ $[-1.1, -0.4]$; *sensor profile corrected TL* %MBE, $M = -2.4\%$ $[-1.8, -2.9]$) and precision (RMSE; *calibrated profile corrected TL*, 2.1%; *sensor profile corrected TL*, 3.9%). *Profile corrected TL* %MBE was reduced in the laser marker when compared to the foreground marker (Fig. 10; mean; laser, -0.18% $[-0.6, 0.3]$; foreground, -1.1% $[-1.6, -0.6]$), however, this was not a significant reduction in bias (wls-GLMM, $p = 0.76$). Error in estimating TL by species was also non-significant (wls-GLMM, $p = 0.88$).

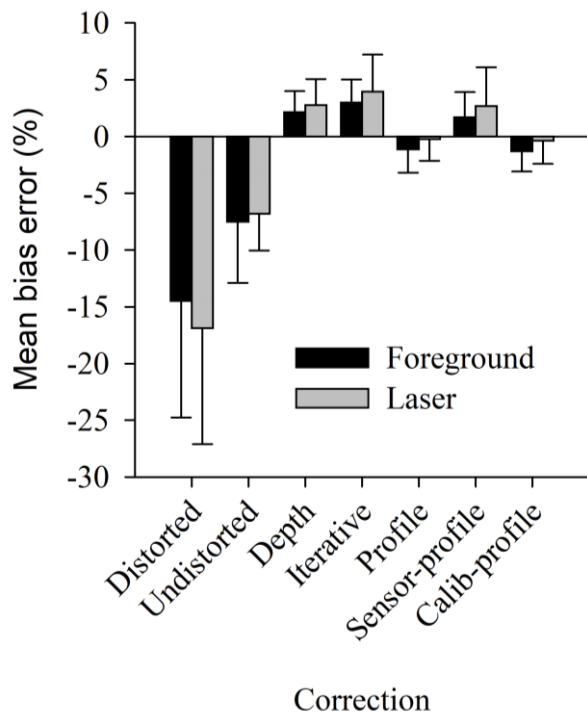


Fig. 10. Species combined percentage mean bias errors from estimated total length of foreground and laser fiducial markers. Standard deviation represented by error bars.

4 Discussion

4.1 Distortion Correction

By applying corrections for geometric lens distortion, the accuracy of length estimates using foreground and parallel laser fiducial markers was significantly reduced in both test fish species. Accuracy was further enhanced by applying increasingly refined corrections to account for the changing distance between the camera and the subject across the surface of the subject. The highest accuracy levels were achieved (%MBE = -0.6 %) when the lens to subject distance was manually measured to mm accuracy, and the TL estimated by iteratively accumulating additional lengths and adding the accumulated sum to the initial length estimate. This level of error is comparable to that observed by Hold *et al.* (2015) who used a fiducial marker to estimate carapace size in crab and lobster where the mean differences between estimated and actual lengths were 0.1 % and 0.6 % respectively. Similar mean differences have been reported when using paired lasers (Deakos 2010, 0.4 % in *Manta alfredi*), or multi-camera systems (Rosen *et al.* 2013 1.0 % in 3 fusiform fish species). The errors observed in length estimates were not significantly different from 0 and equated to 2 mm in 10 cm. Population studies that examine population size-structure typically bin estimates into size classes (Pauly & Morgan, 1987) hence this level of error should not unduly bias biomass catch estimates, size selectivity, or any other size dependent research.

Two approaches were presented to estimate lens to subject distance to correct for parallax errors. Calibration images were shown to be more accurate however, it cannot be assumed this is the general case. The less accurate method calculated lens to subject distance from sensor size in actual units and in pixels. The authors believe the error is likely to have arisen from incorrect manufacturers' figures for actual sensor size and focal length given that actual fiducial marker size, fiducial marker height on the sensor and sensor size in pixels were known

precisely. Empirical verification of which method best estimates lens to subject distance could be justified on a per-camera basis and linear modelling of the error should produce a satisfactory correction.

Lens distortion correction software is available in multiple packages and the mathematics is well understood for tangential and radial distortion (Szeliski, 2010) however, lens distortion correction using OpenCV lens calibration is less well tested. Using this method we reduced RMSE to 0.76 pixels, which equates to submillimetre accuracy at lens to subject distances of between 192 mm and 659 mm. Neuswanger et al. (2016) reported improved correction performance with an extra parameter in the radial distortion model (Szeliski, 2010; Zhang, 2000). OpenCV is released under a 3-clause BSD license allowing the code to be modified, reused and redistributed. This makes OpenCV accessible for incorporation into machine vision pipelines and across diverse operating systems, including smartphones. Other methods of lens distortion correction tend to be in proprietary software released by the camera manufacturers (e.g. GoPro Studio), in photo editing software (e.g. Adobe Photoshop and PTLens), or in scientific software (e.g. MatLab). VidSync (Neuswanger et al., 2016) is an open source package which supports lens calibration however, it has no API and is authored in Objective C, hence can only be executed on Mac OS. In contrast, OpenCV and Python offer greater platform agnosticism, with support across MS Windows, Mac OS, Android, Linux and other platforms.

Hold *et al.* (2015) found that radial distortion was limited by ensuring the subject was centred in the FoV (also see Rodgers *et al.*, 2017). The parallax effect was empirically controlled with a 2nd order linear model with FoV as a predictor. This approach was successful in reducing bias however, empirical modelling is unsuitable where the camera model, lens to subject distance and framing of the subject (and fiducial marker) in the image cannot be prescribed. The model will only make known valid predictions over the quadvariate distribution of focal length,

subject size, FoV (or lens to subject distance) and the subject rotation over which the model was fitted. Hence combining lens calibration with a mechanistic model of parallax effects (as presented), provides a generalisable solution which should be applicable to a wide range of length estimation correction when using fiducial markers.

In this article, tangential distortion was controlled experimentally. However, where the optical axis may not be perpendicular to the subject then tangential distortion must be corrected. OpenCV provides support for calculating the corrective affine transformation and support for identifying checkerboard vertices (or other regular structures). Furthermore, the OpenCV ArUco marker library (Garrido-Jurado, Muñoz-Salinas, Madrid-Cuevas, & Marín-Jiménez, 2014) supports marker detection and predicts the affine transformation required to correct tangential distortion based on the orientation of the marker. Hence, further work should be undertaken to evaluate the effectiveness of correcting for tangential distortion using the OpenCV API.

4.2 Fiducial marker type

The foreground fiducial marker had the same accuracy as paired parallel lasers in the estimation of TL. Both markers were subject to the same underlying causes of error because the mean ALPP across the marker is not the same as the mean ALPP across the dimension of the subject being measured. The background marker provided accurate estimates of TL, even in radially distorted images. This is because; (i) the ALPP of the marker was calculated across the whole length of the subject and so mean ALPP was the same irrespective of any distortions; (ii) when measuring fish length the caudal fin is at the same field depth as the background marker, hence there is only a small parallax error caused by the elevation of the snout above the background marker (which resulted in a small overestimate). Using a background fiducial marker will only be accurate when the length of the fish is not elevated above the distal plane however, we propose the general iterative approach to correct parallax errors can equally be

applied (with adjustments) when using a background marker. As with laser and foreground fiducial markers researchers must ask themselves what may cause the mean ALPP to differ between the marker and the length being measured.

The choice of marker is context-dependent. Foreground and background markers are relatively inexpensive to use but must be positioned close to the fish. Paired lasers can be projected onto a subject from a distance but become difficult to differentiate in intense broad spectrum visible light (e.g. strong sunlight) or where the surface absorbs or diffuses the wavelength of the laser marker. We suggest that environmental conditions can render laser markers difficult to detect using machine vision.

5 Conclusion

The increasing availability and decreasing costs of robust cameras makes them more attractive to ecological and fisheries researchers. We have developed a mechanistic methodology to achieve accurate estimation of morphometric measurements from 2-D images captured with limited control over the equipment. Increasing the accuracy of length estimation from images using software automation could reduce costs and would increase the potential to collect finer grain data in population assessments, particularly—but not exclusively—in citizen science and other volunteer based projects.

6 References

- Bartholomew, D. C., Mangel, C., Alfaro-shigueto, J., Pingo, S., Jimenez, A., Godley, B. J., ... Godley, B. J. (2018). Remote electronic monitoring as a potential alternative to on-board observers in small-scale fisheries. *Biological Conservation*, 219(May 2017), 35–45. <https://doi.org/10.1016/j.biocon.2018.01.003>
- Bicknell, A. W. J., Godley, B. J., Sheehan, E. V., Votier, S. C., & Witt, M. J. (2016). Camera technology for monitoring marine biodiversity and human impact. *Frontiers in Ecology and the Environment*, 14(8), 424–432. <https://doi.org/10.1002/fee.1322>
- Bouchet, P. J., & Meeuwig, J. J. (2015). Drifting baited stereo-videography: a novel sampling tool for surveying pelagic wildlife in offshore marine reserves. *Ecosphere*, 6(8), art137. <https://doi.org/10.1890/ES14-00380.1>
- Chang, S.-K., DiNardo, G., & Lin, T.-T. (2010). Photo-based approach as an alternative method for collection of albacore (*Thunnus alalunga*) length frequency from longline vessels. *Fisheries Research*, 105(3), 148–155. <https://doi.org/10.1016/J.FISHRES.2010.03.021>
- Claassens, L., & Hodgson, A. N. (2018). Gaining insights into in situ behaviour of an endangered seahorse using action cameras. *Journal of Zoology*, 304(2), 98–108. <https://doi.org/10.1111/jzo.12509>
- Costa, C., Loy, A., Cataudella, S., Davis, D., & Scardi, M. (2006). Extracting fish size using dual underwater cameras. *Aquacultural Engineering*, 35(3), 218–227. <https://doi.org/10.1016/J.AQUAENG.2006.02.003>
- Deakos, M. H. (2010). Paired-laser photogrammetry as a simple and accurate system for measuring the body size of free-ranging manta rays *Manta alfredi*. *Aquatic Biology*, 10(1), 1–10. <https://doi.org/10.3354/ab00258>
- Dunbrack, R. L. (2006). In situ measurement of fish body length using perspective-based remote stereo-video. *Fisheries Research*, 82(1–3), 327–331. <https://doi.org/10.1016/J.FISHRES.2006.08.017>
- Faunce, C. H., & Barbeaux, S. J. (2011). The frequency and quantity of Alaskan groundfish catcher-vessel landings made with and without an observer. *ICES Journal of Marine Science*, 68(8), 1757–1763. <https://doi.org/10.1093/icesjms/fsr090>
- Fishbrain. (2018). Fishbrain [Web Page]. Retrieved July 19, 2018, from <https://fishbrain.com/mission/>
- Garrido-Jurado, S., Muñoz-Salinas, R., Madrid-Cuevas, F. J., & Marín-Jiménez, M. J. (2014).

Automatic generation and detection of highly reliable fiducial markers under occlusion. *Pattern Recognition*, 47(6), 2280–2292. <https://doi.org/10.1016/j.patcog.2014.01.005>

Harvey, E. S., Fletcher, D., & Shortis, M. R. (2001). A comparison of the precision and accuracy of estimates of reef-fish lengths made by divers and a stereo-video system. *Fishery Bulletin*, 99(1), 63–71. Retrieved from http://www.geomsoft.com/markss/papers/Harvey_etal2001_comp_precacc.pdf

Hold, N., Murray, L. G., Pantin, J. R., Haig, J. A., Hinz, H., & Kaiser, M. J. (2015). Video capture of crustacean fisheries data as an alternative to on-board observers. *ICES Journal of Marine Science*, 72(6), 1811–1821. <https://doi.org/10.1093/icesjms/fsv030>

Hyder, K., Townhill, B., Anderson, L. G., Delany, J., & Pinnegar, J. K. (2015). Can citizen science contribute to the evidence-base that underpins marine policy? *Marine Policy*, 59(0), 112–120. <https://doi.org/10.1016/j.marpol.2015.04.022>

IBM Corp. (2011). IBM SPSS Statistics for Windows. Released 2011. [Computer Program], Armonk, NY: IBM. Retrieved from <https://www.ibm.com/uk-en/products/spss-statistics>

ICES. (2017). *ICES WGRFS Report 2017. Report of the Working Group on Recreational Fisheries Surveys (WGRFS) 12-16 June 2017* [Report]. Azores, Portugal. Retrieved from https://www.ices.dk/sites/pub/Publication Reports/Expert Group Report/SSGIEOM/2017/WGRFS/wgrfs_2017.pdf

Jaquet, N. (2006). A simple photogrammetric technique to measure sperm whales at sea. *Marine Mammal Science*, 22(4), 862–879. <https://doi.org/10.1111/j.1748-7692.2006.00060.x>

Jeong, S. J., Yang, Y. S., Lee, K., Kang, J. G., & Lee, D. G. (2013). Vision-based automatic system for non-contact measurement of morphometric characteristics of flatfish. *Journal of Electrical Engineering and Technology*, 8(5), 1194–1201. <https://doi.org/10.5370/JEET.2013.8.5.1194>

Loy, A., Boglione, C., Gagliardi, F., Ferrucci, L., & Cataudella, S. (2000). Geometric morphometrics and internal anatomy in sea bass shape analysis (*Dicentrarchus labrax* L., Moronidae). *Aquaculture*, 186(1–2), 33–44. [https://doi.org/10.1016/S0044-8486\(99\)00366-X](https://doi.org/10.1016/S0044-8486(99)00366-X)

National Oceanic and Atmospheric Administration. (2015a). *A Cost Comparison of At-Sea Observers and Electronic Monitoring for a Hypothetical Midwater Trawl Herring / Mackerel Fishery*. [Report]. Retrieved from https://www.greateratlantic.fisheries.noaa.gov/fish/em_cost_assessment_for_gar_herring_150904_v6.pdf

- National Oceanic and Atmospheric Administration. (2015b). *A Preliminary Cost Comparison of At-sea Monitoring and Electronic Monitoring for a Hypothetical Groundfish Sector* [Report]. Retrieved from https://www.greateratlantic.fisheries.noaa.gov/stories/2015/september/em_cost_assessment_for_gar_multispecies_2015_06_10.pdf
- Neuswanger, J. R., Wipfli, M. S., & Rosenberger, A. E. (2016). Measuring fish and their physical habitats : Versatile 2-D and 3-D video techniques with user-friendly software. *Canadian Journal of Fisheries and Aquatic Sciences*, 13(June), 1–48. <https://doi.org/10.1139/cjfas-2016-0010>
- Nguyen, T. X., Winger, P. D., Legge, G., Dawe, E. G., & Mullett, D. R. (2014). Underwater observations of the behaviour of snow crab (*Chionoecetes opilio*) encountering a shrimp trawl off northeast Newfoundland. *Fisheries Research*, 156, 9–13. <https://doi.org/10.1016/J.FISHRES.2014.04.013>
- OpenCV team. (2018). OpenCV: Camera Calibration and 3D Reconstruction [Web Page]. Retrieved April 23, 2018, from https://docs.opencv.org/master/d9/d0c/group__calib3d.html
- Pauly, D., & Morgan, G. R. (1987). Length-Based Methods in Fisheries Research. In *The Theory and Application of Length-Based Stock Assessment Methods* (pp. 1–459). Mazara del Vallo, Sicily.
- Poli, B. M., Parisi, G., Zampacavallo, G., Mecatti, M., Lupi, P., Gualtieri, M., & Franci, O. (2001). Quality outline of European sea bass (*Dicentrarchus labrax*) reared in Italy: Shelf life, edible yield, nutritional and dietetic traits. *Aquaculture*, 202(3–4), 303–315. [https://doi.org/10.1016/S0044-8486\(01\)00780-3](https://doi.org/10.1016/S0044-8486(01)00780-3)
- Rogers, T. D., Cambiè, G., & Kaiser, M. J. (2017). Determination of size, sex and maturity stage of free swimming catsharks using laser photogrammetry. *Marine Biology*, 164(11), 1–11. <https://doi.org/10.1007/s00227-017-3241-7>
- Rohlf, F. J., & Marcus, L. F. (1993). A revolution in morphometrics. *Trends in Ecology & Evolution*, 8(4), 129–132.
- Rosen, S., Jørgensen, T., Hammersland-White, D., & Holst, J. C. (2013). DeepVision: a stereo camera system provides highly accurate counts and lengths of fish passing inside a trawl. *Canadian Journal of Fisheries and Aquatic Sciences*, 70(10), 1456–1467. <https://doi.org/10.1139/cjfas-2013-0124>
- Schmid, K., Reis-Filho, J. A., Harvey, E. S., & Giarrizzo, T. (2017). Baited remote underwater video as a promising nondestructive tool to assess fish assemblages in

- clearwater Amazonian rivers: testing the effect of bait and habitat type. *Hydrobiologia*, 784(1), 93–109. <https://doi.org/10.1007/s10750-016-2860-1>
- Schneider, C. A., Rasband, W. S., & Eliceiri, K. W. (2012). NIH Image to ImageJ: 25 years of image analysis. *Nature Methods*, 9(7), 671–675. Retrieved from <http://www.ncbi.nlm.nih.gov/pubmed/22930834>
- Struthers, D. P., Danylchuk, A. J., Wilson, A. D. M., & Cooke, S. J. (2015). Action cameras: Bringing aquatic and fisheries research into view. *Fisheries*, 40(10), 502–512. <https://doi.org/10.1080/03632415.2015.1082472>
- Szeliski, R. (2010). *Computer Vision: algorithms and applications*. [Book], Springer Science & Business Media. <https://doi.org/10.1007/978-1-84882-935-0>
- Tulli, F., Balenovic, I., Messina, M., & Tibaldi, E. (2009). Biometry traits and geometric morphometrics in sea bass (*Dicentrarchus labrax*) from different farming systems. *Italian Journal of Animal Science*, 8(SUPPL. 2), 881–883. <https://doi.org/10.4081/ijas.2009.s2.881>
- van Helmond, A. T. M., Chen, C., & Poos, J. J. (2017). Using electronic monitoring to record catches of sole (*Solea solea*) in a bottom trawl fishery. *ICES Journal of Marine Science*, 74(5), 1421–1427. <https://doi.org/10.1093/icesjms/fsw241>
- Venturelli, P. A., Hyder, K., & Skov, C. (2017). Angler apps as a source of recreational fisheries data : opportunities , challenges and proposed standards. *Fish and Fisheries*, 18, 578–595. <https://doi.org/10.1111/faf.12189>
- VideoLAN. (2018). VLC media player. [Computer Program], VideoLAN. Retrieved from <https://www.videolan.org/vlc/index.en-GB.html>
- White, D. J., Svelling, C., & Strachan, N. J. C. (2006). Automated measurement of species and length of fish by computer vision. *Fisheries Research*, 80(2–3), 203–210. <https://doi.org/10.1016/j.fishres.2006.04.009>
- Zhang, Z. (2000). A flexible new technique for camera calibration. *IEEE Transactions on Pattern Analysis and Machine Intelligence*, 22(11), 1330–1334. <https://doi.org/10.1109/34.888718>

7 Funding

This work was supported by the Fisheries Society of the British Isles under a PhD Studentship granted to GGM. KH was supported by Cefas Seedcorn (DP227AE).

526 **8 Supplementary Materials**

527 Supplementary material is available at ICES JMS online; (i) Supplementary materials A, B
528 and C are code listings (Python 3.5) of the core functions used for (S1) lens calibration; (S2)
529 calculate the standardised mean subject width; (S3) Table 1 variable calculations.

530 **9 Competing Interests**

531 No competing interests to declare